rpth
research & practice
in thrombosis & haemostasis

ORIGINAL ARTICLE

Activation of coagulation FXI promotes endothelial inflammation and amplifies platelet activation in a nonhuman primate model of hyperlipidemia

Tia C. L. Kohs[1] | Helen H. Vu[1] | Kelley R. Jordan[1] | Iván Parra-Izquierdo[1] 🐦 | Monica T. Hinds[1] | Joseph J. Shatzel[1,2] 🐦 | Paul Kievit[3] | Terry K. Morgan[4] | Samuel Tassi Yunga[1,5] | Thuy T. M. Ngo[1,5,6] 🐦 | Joseph E. Aslan[1,7,8] 🐦 | Michael Wallisch[1,9] | Christina U. Lorentz[1,9] | Erik I. Tucker[1,9] 🐦 | David Gailani[10] | Jonathan R. Lindner[11] 🐦 | Cristina Puy[1] | Owen J. T. McCarty[1,2]

[1]Department of Biomedical Engineering, Oregon Health & Science University, Portland, Oregon, USA

[2]Division of Hematology and Oncology, Oregon Health & Science University, Portland, Oregon, USA

[3]Division of Cardiometabolic Health, Oregon National Primate Research Center, Oregon Health & Science University, Beaverton, Oregon, USA

[4]Department of Pathology and Laboratory Medicine, Oregon Health & Science University, Portland, Oregon, USA

[5]Cancer Early Detection Advanced Research Center, Knight Cancer Institute, Oregon Health & Science University, Portland, Oregon, USA

[6]Department of Molecular and Medical Genetics, Oregon Health & Science University, Portland, Oregon, USA

[7]Knight Cardiovascular Institute, School of Medicine, Oregon Health & Science University, Portland, Oregon, USA

[8]Department of Chemical Physiology and Biochemistry, Oregon Health & Science University, Portland, Oregon, USA

[9]Aronora, Inc, Portland, Oregon, USA

[10]Department of Pathology, Microbiology and Immunology, Vanderbilt University Medical Center, Nashville, Tennessee, USA

[11]Division of Cardiovascular Medicine and Robert M. Berne Cardiovascular Research Institute, University of Virginia, Charlottesville, Virginia, USA

Abstract

Background: Hyperlipidemia is associated with chronic inflammation and thromboinflammation. This is an underlying cause of several cardiovascular diseases, including atherosclerosis. In diseased blood vessels, rampant thrombin generation results in the initiation of the coagulation cascade, activation of platelets, and endothelial cell dysfunction. Coagulation factor (F) XI represents a promising therapeutic target to reduce thromboinflammation, as it is uniquely positioned at an intersection between inflammation and thrombin generation.

Objectives: This study aimed to investigate the role of FXI in promoting platelet and endothelial cell activation in a model of hyperlipidemia.

Methods: Nonhuman primates (NHPs) were fed a standard chow diet (lean, $n = 6$) or a high-fat diet (obese, $n = 8$) to establish a model of hyperlipidemia. Obese NHPs were intravenously administered a FXI blocking antibody (2 mg/kg) and studied at baseline and at 1, 7, 14, 21, and 28 days after drug administration. Platelet activation and inflammatory markers were measured using fluorescence-activated cell sorting or enzyme-linked immunosorbent assay. Molecular imaging was used to quantify vascular cell adhesion molecule 1 (VCAM-1) expression at the carotid bifurcation.

Results: Obese NHPs demonstrated increased sensitivity for platelet P-selectin expression and phosphatidylserine exposure in response to platelet GPVI or PAR agonists compared with lean NHPs. Obese NHPs exhibited elevated levels of C-reactive protein, cathepsin D, and myeloperoxidase compared with lean NHPs. Following pharmacological inhibition of FIX activation by FXIa, platelet priming for activation by GPVI or PAR agonists, C-reactive protein levels, and endothelial VCAM-1 levels were reduced in obese NHPs.

rpth
research & practice
in thrombosis & haemostasis

Correspondence

Tia C. L. Kohs, Department of Biomedical Engineering, Oregon Health & Science University, 3303 S Bond Avenue, Portland, OR 97239, USA.
Email: kohst@ohsu.edu

Handling Editor: Dr Henri Spronk.

Conclusion: FXI activation promotes the proinflammatory phenotype of hyperlipidemia by priming platelet activation and inciting endothelial cell dysfunction.

KEYWORDS
atherosclerosis, hyperlipidemia, inflammation, platelets, thrombin

Essentials

- Hyperlipidemia and obesity are associated with chronic vascular inflammation and clotting.
- We studied the effect of diet-induced obesity on platelet sensitivity and inflammatory markers.
- Targeting coagulation factor XI reduced platelet priming for activation and inflammation.
- Our study demonstrates that factor XI activation promotes vascular dysfunction in hyperlipidemia.

1 | INTRODUCTION

Thromboinflammation associated with hyperlipidemia is an underlying cause of cardiovascular diseases, including atherosclerosis [1]. In the setting of atherosclerosis, lipid accumulation within the blood vessel walls prompts endothelial cell dysfunction [2–4]. Concomitantly, select chemokines and chemoattractants are upregulated and secreted, which results in aberrant recruitment of leukocytes into the intima [2,4]. Circulating lipoproteins are readily oxidized and internalized by macrophages, thereby generating foam cells in the nascent atheroma and secreting additional inflammatory cytokines and reactive oxygen species [5]. Mature plaques with a necrotic core form following the accumulation of dying macrophages. The rupture of these plaques is highly thrombogenic and is a common cause of myocardial infarction or stroke [6,7].

Thrombin generation is central to the homeostasis and regulation of barrier function and protection against vessel damage. In the setting of diseased blood vessels, rampant acceleration and propagation of thrombin generation results in 1) occlusive thrombus formation, 2) onset of inflammation, and 3) deleterious loss of endothelial barrier function [8]. By way of amplifying thrombin generation, coagulation factor (F) XI has been shown to play a detrimental role in promoting thromboinflammation, in part by creating a thrombin amplification loop. FXI is activated by thrombin, which by then activates FIX, and FXIa feeds forward to generate more thrombin [9]. Yet, the enzymatic function of FXIa has been shown to extend beyond an exclusive partnership with FIX. These functions range from degradation of inhibitors of thrombin generation (eg, tissue factor pathway inhibitor) to activation of "upstream" members of the coagulation cascade (eg, FXII) [10–12]. In fact, it has become apparent that FXIa acts on a litany of substrates to amplify local thrombin generation, platelet activation, and endothelial cell barrier function, thereby serving as a valued member in the maintenance of homeostasis [13]. In the setting of hyperlipidemia, these processes are imbalanced, creating a pathologic thromboinflammatory phenotype.

The multifaceted function of FXIa has provided the rationale for testing if inhibition of FXI activation or FXIa activity is anti-inflammatory in addition to being antithrombotic. Indeed, it has been observed that FXI inhibition improves outcomes in *in vivo* mouse models of atherosclerosis [14], sepsis [15–17], ischemic stroke, and myocardial infarction [18,19]. Moreover, inhibition of either FXII or FXI activation prevented an acute inflammatory response, platelet consumption, and reduced markers of endothelial dysfunction in a baboon model of systemic inflammatory response syndrome [12,20,21]. This anti-inflammatory signature of FXI inhibition was observed in clinical trials, wherein a reduction in C-reactive protein levels was observed in end-stage renal disease patients on chronic hemodialysis on a FXI inhibitor [22]. Based on these observations, we interrogated if pharmacological inhibition of FXI activation by FXIIa and of FIX activation by FXIa with the anti-FXI antibody, humanized 1A6 (h1A6), would reduce thromboinflammation in a nonhuman primate model of hyperlipidemia.

2 | METHODS

2.1 | Reagents

Crosslinked collagen-related peptide (CRP-XL) was obtained from Dr Richard Farndale (Cambridge University). Adenosine diphosphate (ADP) was purchased from Sigma-Aldrich. Thrombin receptor activator peptide 6 (TRAP-6) was purchased from Tocris Bioscience. The activated partial thromboplastin time (aPTT) reagent and prothrombin time (PT) Dade Innovin were purchased from Thermo Fisher Scientific and Siemens Healthcare Diagnostics, respectively. The polystyrene bead standards used for nanoscale flow cytometry, Megamix-Plus FSC and Megamix-Plus SSC, were purchased from BioCytex.

2.2 | Antibodies

The mouse antihuman PE CD62P (P-selectin) antibody used for flow cytometry was obtained from BD Biosciences. The fluorescein iso-thiocyanate (FITC) bovine lactadherin used for flow cytometry was

obtained from Haematologic Technologies and BioLegend. The mouse antihuman monoclonal IgG1 against VCAM-1 (1.G11B1) used for contrast-enhanced ultrasound (CEU) molecular imaging was obtained from Bio-Rad Antibodies.

2.3 | Generation of anti-FXI monoclonal antibody

The anti-FXI monoclonal antibody, 1A6, was generated as previously described [23]. This antibody binds to the apple 3 domain of FXI, and blocks FXIIa-mediated activation of FXI as well as FXIa-mediated activation of FIX and FV. Note that although 1A6 does not inhibit feedback activation of FXI by thrombin, and thus does not block the generation of FXIa, the downstream enzymatic action of FXIa on FIX in particular is eliminated. The humanized form of the antibody, h1A6 (BAY 1831865), was a generous gift from Bayer AG.

2.4 | Nonhuman primate (NHP) model of hyperlipidemia

All rhesus macaque (*Macaca mulatta*) studies were approved by the Oregon Health & Science University Institutional Animal Care and Use Committee (IP00002332). The rhesus macaques were housed and cared for by the Oregon National Primate Research Center (ONPRC) at Oregon Health & Science University.

Adult male rhesus macaques were placed in lean (n = 6) and obese (n = 8) cohorts. The lean cohort was fed a standard diet (58% carbohydrates, 27% protein, and 15% fat by caloric content; Lab-Diet 5L0P, Purina Mills), whereas the obese cohort was fed a high-fat diet (45% carbohydrates, 18% protein, and 36% fat by caloric content; LabDiet 5L0P, Purina Mills) for an average of 7.6 ± 1.6 years.

From the obese cohort, 5 rhesus macaques were administered the humanized anti-FXI monoclonal IgG 1A6 (h1A6) at 2 mg/kg on day 0. This dose was selected based on prior works showing that 1A6 administered to a baboon at 2 mg/kg inhibited >99% of FXI activity for at least 10 days [23]. Thus, to ensure that maximal inhibition was maintained throughout a 28-day time course, we administered an additional maintenance dose of h1A6 (2 mg/kg) on day 14 following blood collection. Hematological analyses were performed at designated study intervals (Supplementary Figure S1).

2.5 | Blood collection

Venous blood samples were collected by venipuncture into 3.2% sodium citrate or EDTA vacutainers prior to administration of h1A6 at time = 0 (day 0) and at days 1, 7, 14, 21, and 28 following h1A6 treatment. Platelet-poor plasma (PPP) was obtained by centrifugation of whole blood for 10 minutes at 2000 *g*, removal of the supernatant, and centrifugation of the remaining plasma for 10 minutes at 2000 *g*.

Plasma samples that were not immediately used for analyses were banked at −80 °C for batch testing.

2.6 | Hematological analysis for complete blood counts and lipid levels

Whole blood samples were analyzed for lipid levels and complete blood counts by the Clinical Pathology Laboratory at the ONPRC using an ABX Pentra 400 Clinical Chemistry System (Horiba Medical).

2.7 | Plasma clotting assays and quantification of coagulation factor activation

Clotting times were measured in PPP isolated from whole blood anticoagulated with 3.2% sodium citrate. In brief, PPP was incubated with the aPTT reagent for 3 minutes at 37 °C. Clotting was initiated by the addition of $CaCl_2$ (25 mM) and measured using a KC4 Coagulation Analyzer (Bray Co). To measure the PT, clotting of PPP was initiated by the equivolume addition of Dade Innovin reagent.

FXIIa–antithrombin (AT), FXIa–AT, and T–AT complexes were quantified in PPP isolated from whole blood anticoagulated with EDTA as described previously [12,20]. FXIa–AT and T-AT standards were prepared by incubating FXIa (1 μM) or thrombin (1 μM) with antithrombin (5 μM), EDTA (1 mM), and heparin (5 U/mL) for 2 hours at 37 °C. Standards were defined as 1 μM of protease–antithrombin complex [24]. Terminal complement complex (C5b-9) was quantified as described previously [25].

2.8 | Flow cytometry for platelet activity

The platelet activation state was assessed by measuring α-granule secretion and phosphatidylserine (PS) expression by flow cytometry. Whole blood anticoagulated with 3.2% sodium citrate was diluted in modified HEPES-Tyrode buffer (1:4). Platelet P-selectin (CD62P) expression was used as a marker for α-granule secretion and was analyzed with an anti-CD62P PE (1:20) antibody at baseline or following stimulation with the GPVI agonist CRP-XL (0.3, 1.0 μg/mL), ADP (1.0, 3.0 μM), or a PAR-1 agonist TRAP-6 (30, 100 μM) for 20 minutes at 37 °C. PS exposure on the membrane was used as a marker of a procoagulant platelet phenotype and analyzed with FITC bovine lactadherin (1:10) in the presence of a combination of CRP-XL (1.0 μg/mL) and TRAP-6 (100 μM). To stop reactions, samples were diluted with paraformaldehyde (2%). Flow cytometry was performed on a FACSCanto II (BD Biosciences).

Data were analyzed using FlowJo software (version 10.7.1). To measure platelet activation, platelet populations were first identified by logarithmic signal amplification for forward (FSC) and side scatter (SSC). Using a within-subject design, with each animal serving as its own control to minimize individual variations, data were presented as percentage of platelets expressing CD62P or PS on the membrane.

2.9 | Hematological analysis for inflammatory biomarkers

NHP EDTA–plasma samples were analyzed for inflammatory biomarkers by the Endocrine Technologies Core (ETC) at the ONPRC. Plasma samples were analyzed for C-reactive protein using an enzyme-linked immunosorbent assay kit (ELISA, ALPCO) following the manufacturer's instructions. The assay range was 0.95 to 150 ng/mL and intra-assay CV was 2.7%. The interassay CV for the C-reactive protein ELISA was 11.1%. Plasma samples were also analyzed for cathepsin D, myeloperoxidase, and soluble vascular cell adhesion molecule-1 (VCAM-1) using a custom Luminex panel (Millipore Sigma HNDG3MAG-36K). The analysis was performed following the manufacturer's instructions. Briefly, 25 μL of each plasma sample was diluted in assay diluent and incubated overnight with antibody-coated, fluorescent-dyed capture microspheres specific for each analyte, followed by incubation with detection antibodies and streptavidin-phycoerythrin. Washed microspheres with bound analytes were resuspended in reading buffer and analyzed on a Milliplex LX-200 Analyzer (EMD Millipore) bead sorter with XPonent Software version 3.1 (Luminex). Data were calculated using Milliplex Analyst software version 5.1 (EMD Millipore). Intra-assay CVs were as follows: cathepsin D (5.6%), MPO (9.0%), and sVCAM-1 (8.0%). Since all the samples were analyzed in a single assay, no interassay variation was calculated for this study.

2.10 | Nanoparticle tracking analysis

Total particle concentrations in EDTA–plasma samples were measured by nanoparticle tracking analysis using the ZetaView PMX-420 instrument (Particle Metrix) according to manufacturer guidelines. The instrument was calibrated daily using 100-nm alignment particles supplied by Particle Metrix. Plasma samples were diluted 10,000-fold in 0.1-μm–filtered PBS. Settings such as a camera sensitivity of 70% and a frame rate of 30 Hz were selected based on manufacturer recommendations and maintained constant through all runs. Recorded concentrations were adjusted for dilution factor to obtain the particle concentration in the original undiluted plasma and expressed as particles per milliliter.

2.11 | Nanoscale flow cytometry of extracellular vesicles

Nanoscale flow cytometry imaging and counting of stained extracellular vesicles (EVs) were performed as previously described [26–28]. Briefly, PPP was isolated from whole blood anticoagulated with EDTA and was obtained by centrifugation of whole blood for 10 minutes at 2500 g, removal of the supernatant, and centrifugation of the remaining plasma for 10 minutes at 2500 g. EVs were stained with an anti-CD62P APC (1:100), anti-CD41 FITC (1:500), anti-CD41 APC (1:2000), anti-CD9 PE (1:100), or anti-CD31 BV421 (1:1000) antibody

for 1 hour at RT. Samples were then diluted at a ratio of 1:200 with 200-nm bead buffer (fluorescence-activated cell sorting 200-nm beads in PBS) to avoid coincident events and keep the abort rate at <10%. The 200-nm bead sample dilution buffer was used to provide both an internal relative size and volume of sample tested standard for all stained samples. Megamix (100-900 nm, GFP-labeled polystyrene beads) and molecules of equivalent soluble fluorophore beads for each fluorophore conjugate were also used to standardize instrument settings. Flow cytometry was performed on a FACSAria Fusion (BD Biosciences) with a ZenPure PureFlow Mini Capsule PES 0.1-μm filter.

Relative EV sizes were approximated by comparing EV SSC with polystyrene beads and assuming the refractive index of small EVs to be >1.5 and large EVs to be closer to 1.4. Positive antibody staining was used to distinguish EVs from other unlabeled, similarly sized nanoparticles (eg, lipoproteins and nonspecific cell fragments). The expression of CD62P$^+$/CD41$^+$/CD9$^+$ and CD31$^+$/CD41$^-$ expression were used as markers for EVs derived from activated platelets and endothelial cells, respectively. Stained PBS, conjugated isotype controls, and unstained plasma samples served as negative controls. Data were collected based on uniform 200 nm bead sample dilution buffer bead counts, which provided test volumes for each sample. Data were reported as gated events per microliter of starting plasma. The mean of duplicate experiments for each sample was employed for statistical analyses. Data were log-transformed to adjust for geometric variance with the mean.

2.12 | Targeted molecular imaging agent preparation

Lipid-shelled decafluorobutane microbubbles targeted to endothelial VCAM-1 were prepared as previously described [29–31]. Briefly, the microbubbles were derived by sonicating a gas-saturated aqueous suspension of distearoylphosphatidylcholine (2 mg/mL), polyoxyethylene 40 stearate (1 mg/mL), and distearoylphosphatidylethanolamine–PEG (2000) biotin (0.4 mg/mL). Targeting was achieved using a streptavidin bridge to conjugate a biotinylated anti–VCAM-1 antibody (1.G11B1) to the microbubble surface. The cross reactivity of the VCAM-1 antibody with macaque epitopes was evaluated by immunohistochemistry of banked spleen and carotid artery samples from animals that were fed a high-fat diet for 2 years [30]. Control microbubbles were unconjugated with no targeting ligand. Electrozone sensing was used to measure microbubble concentration and to ensure similar size distribution between the agents for each experiment (Multisizer III, Beckman Coulter).

2.13 | Contrast-enhanced ultrasound molecular imaging

CEU molecular imaging at the carotid bifurcation was used to measure endothelial VCAM-1 as a marker of endothelial cell activation before

and after treatment with h1A6, as previously described [29–31]. In brief, we performed longitudinal-axis imaging at the carotid bifurcation using multipulse, contrast-specific imaging at 7 MHz, a mechanical index of 1.9, a dynamic range of 55 dB, and a frame rate of 1 Hz (Sequoia, Siemens Medical Imaging). Microbubbles targeted to endothelial VCAM-1 (1×10^8) were intravenously injected and the ultrasound was paused for 1 minute before locating the carotid artery. We located the carotid artery using 2D ultrasound at low power (mechanical index < 0.10) and activated contrast-specific imaging for several frames. The signal for retained microbubbles was quantified by taking a digital average of the first 2 frames acquired. To distinguish the signal from microbubbles freely circulating, we subtracted several averaged frames that were acquired after >5 destructive pulse sequences (mechanical index: 1.3). Data from regions of interest at the near and far walls of the common carotid artery were averaged.

2.14 | Statistical analysis

Data were tested for normality and sphericity using Shapiro–Wilk and F-tests. Two group data that were normally distributed with equal SDs were analyzed by an unpaired t-test. If the SDs were not equal, then Welch's correction was applied. Data that were not normally distributed were analyzed by a Mann–Whitney test. For ≥3 groups, normally distributed data were analyzed by repeated measures one-way ANOVA with a Dunnett's post-hoc test. Data that were not normally distributed were analyzed by a Friedman test with a Dunn's post-hoc test. Statistical significance was considered for $P < .05$. For all experiments, n indicates the number of independent experiments performed. Statistical analyses were performed using GraphPad Prism 9.

3 | RESULTS

3.1 | Effects of diet-induced hyperlipidemia on platelet activity and thrombin generation

We first sought to examine biomarkers of platelet activation and coagulation factor activation in a model of diet-induced hyperlipidemia. When platelets are activated, the contents of their granules, including P-selectin and ADP, which are stored in platelet alpha and dense granules, respectively, are translocated to the platelet surface [32,33]. Therefore, for both obese and lean cohorts, we identified the platelet population using forward vs side scatter (Figure 1A), and quantified P-selectin expression at baseline as well as in response to subthreshold concentrations of platelet agonists. For these experiments, we used agonists that signal downstream of immunotyrosine activation motif- or G-protein–coupled receptor (GPCR)–linked receptors, GPVI or PAR-1, respectively. While the baseline level of platelet activation was equivalent for both lean and obese cohorts, hyperlipidemia primed platelet activation in response to the GPVI agonist (CRP-XL) or PAR-1 agonist (TRAP-6), as evidenced by a substantial increase in platelet P-selectin expression observed in the

obese cohort compared to the lean cohort at an equivalent dose of agonist (Figure 1B, D). Platelet P-selectin expression in response to ADP was variable and insensitive to hyperlipidemia (Figure 1C).

When platelets become activated, intracellular signaling events facilitate PS exposure on the platelet surface. These processes confer a procoagulant scaffold for coagulation factors to assemble a requisite step for thrombin generation and subsequent fibrin formation [34,35]. Thus, systemic platelet coagulability was measured by quantifying PS exposure in response to agonists that signal through GPVI and PAR-1. We found that agonist-induced PS expression levels were elevated in NHP platelets on a high-fat diet compared to platelets from NHPs on a standard chow diet (Figure 1E). Taken together, these results confirm that hyperlipidemia increases the sensitivity of platelets for activation by either GPVI or PAR-1 agonists.

We next examined the effect of hyperlipidemia on coagulation factor activity. We did not observe any differences in aPTT or PT in plasma from the obese or lean cohorts (Figure 2A, B). The level of T-AT complexes were insensitive to diet-induced hyperlipidemia (Figure 2D). However, when profiling the procoagulant phenotype of our obese NHP cohort, we found an increase in FXIa–AT complexes at baseline in the obese cohort (Figure 2C).

3.2 | Effects of diet-induced hyperlipidemia on complete blood counts and lipid levels

Hematological analyses showed that relative to the lean controls, NHPs with diet-induced hyperlipidemia had significantly higher levels of hemoglobin, hematocrit, and red blood cells; interestingly, however, the obese NHPs showed a reduction in white blood cells (Supplementary Table S1). On biochemical analysis, obese NHPs also had elevated levels of alanine transaminase, chloride, total cholesterol, low-density lipoprotein and high-density lipoprotein relative to lean NHPs (Supplementary Table S2). These findings are in line with previous studies comparing lean vs obese NHPs [30,36].

3.3 | Effects of diet-induced hyperlipidemia on inflammation

Systemic inflammation is a hallmark of hyperlipidemia and is accompanied by the upregulation of cytokines and the release of growth factors [37,38]. Accordingly, we measured inflammatory markers known to contribute to plaque instability and the inflammatory tone of atherosclerotic lesions. Confirming the findings from our previous study where NHPs were transitioned to a high-fat diet [30], an increase in plasma levels of C-reactive protein levels was observed in the obese cohort as compared to the lean animals (Figure 3A). Cathepsin D and myeloperoxidase levels also increased in obese NHPs compared to lean NHPs (Figure 3B, C). Complement activation, as measured by levels of C5b-9–soluble terminal complement complex, was elevated in the setting of hyperlipidemia (Figure 3D). While the release of EVs is reflective of a proinflammatory state, we did not
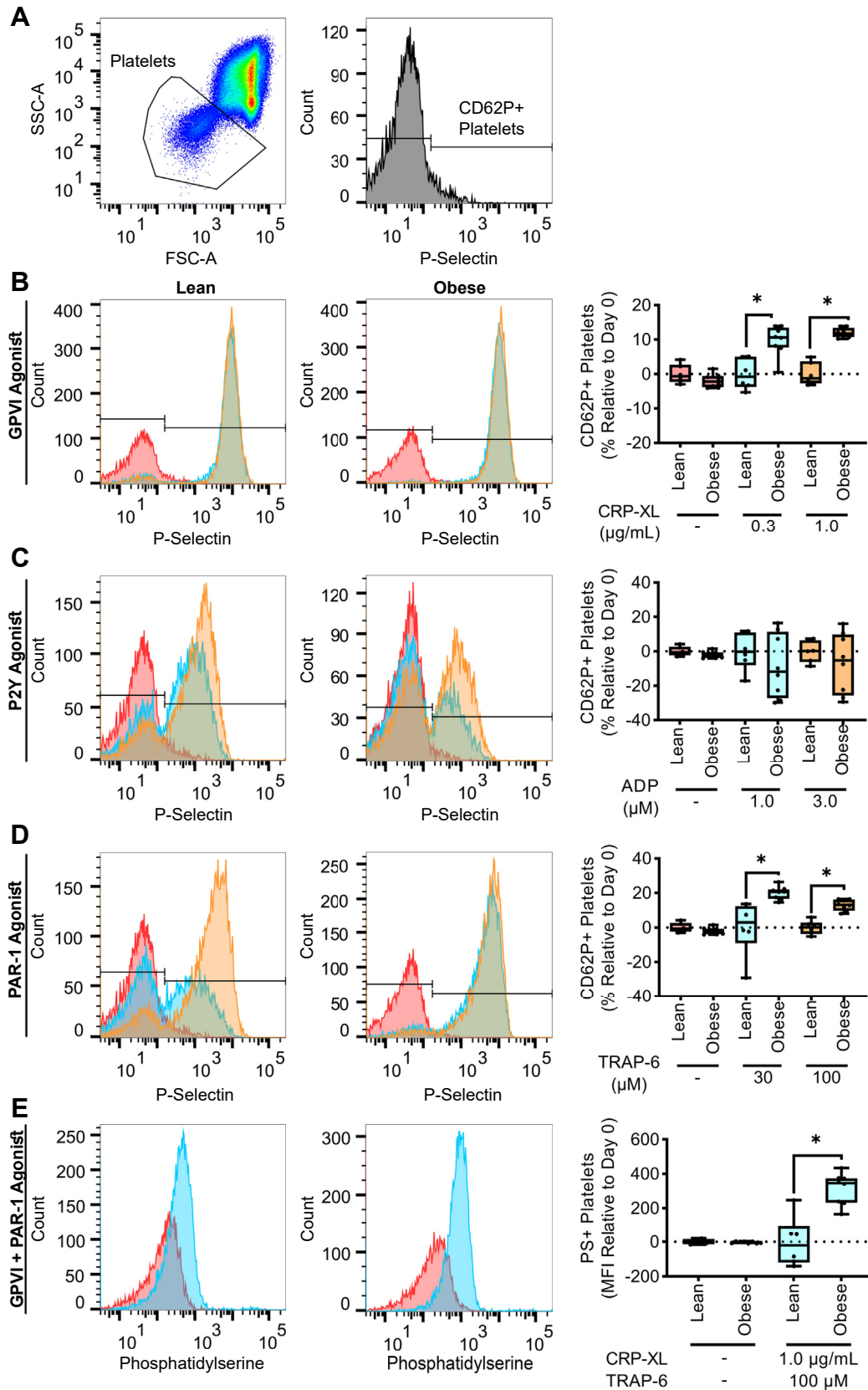
FIGURE 1 Hyperlipidemia primes platelet activation by GPVI or PAR-1 agonists. The platelet population was identified using forward vs side scatter (FSC-A vs SSC-A) gating (A). Whole blood samples from NHPs on a standard chow diet (*n* = 6, lean) or NHPs on a high-fat diet (*n* = 8, obese) were stained with an anti-CD62P PE antibody (B–D) or FITC bovine lactadherin (E). Samples were then stimulated with a GPVI agonist (0.3, 1.0 μg/mL), a P2Y agonist (1.0, 3.0 μM), or a PAR-1 agonist (30, 100 μM). Flow cytometry was used to measure the platelet surface

observe any differences in total EVs, or endothelial (CD31⁺/CD41⁻) or activated platelet (CD62P⁺/CD41⁺/CD9⁺) EV subset particle count, between obese and lean cohorts (Figure 3E–G). These data confirmed that hyperlipidemia increased select markers of inflammation, including C-reactive protein, and the complement system in our NHP model.

3.4 | Effects of pharmacological targeting of FXI on the thromboinflammatory phenotype of hyperlipidemia

As hyperlipidemia was associated with an increase in circulating markers of FXI activation in our model, we evaluated if pharmacological targeting of FXI would provide an antiplatelet and anti-inflammatory benefit. We first confirmed that aPTT clotting times increased following treatment of obese primates with the anti-FXI antibody, h1A6, which inhibits FXI activation by FXIIa as well as FIX and FV activation by FXIa (Figure 4A). Conversely, h1A6 did not affect PT clotting times, confirming that this antibody does not affect the extrinsic pathway of coagulation (Figure 4B). Along these lines, h1A6 was unable to reduce the degree of activated FXI in the obese primate cohort, in line with the fact that this antibody does not prevent thrombin-mediated activation of FXI (Figure 4C). Likewise, we did not observe a reduction in T-AT levels in the presence of h1A6 (Figure 4D).

We next examined the effect of FXI inhibition on platelet reactivity in our model of hyperlipidemia. As shown in Figures 5A, C, the increase in P-selectin expression in responses to GPVI or PAR-1 agonists was diminished after 1 day of treatment with the FXI antibody, h1A6, relative to baseline (day 0). These findings suggest that the sensitization of platelets for activation in the setting of hyperlipidemia was reversed by a FXI inhibitor. Yet, this inhibitory effect was only seen at the 24-hour timepoint, while changes in PS exposure at 24 hours in the presence of the FXI mAb, h1A6, were not statistically significant (Figure 5D). Platelet P-selectin expression in response to ADP stimulation remained varied and was largely insensitive to the presence of hA16 (Figure 5B).

Additional hematological analyses showed that there was a significant increase in white blood cells and lymphocytes after 1 day of treatment with the FXI antibody, h1A6, relative to baseline (day 0). This was followed by later increases in monocytes, platelets, red cell distribution width, glucose, and triglycerides and a decrease in aspartate aminotransferase at day 7 (Supplementary Tables S1 and S2). However, note that there were substantial variations in these markers over the study period.

We next evaluated if pharmacological targeting of FXI would reduce the inflammatory phenotype observed in our diet-induced
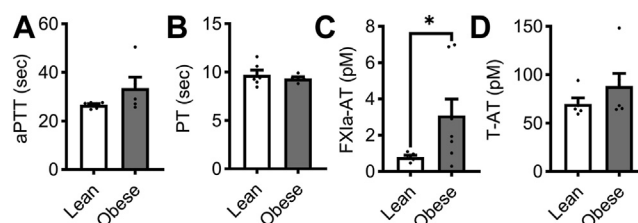

FIGURE 2 Levels of activated FXI were elevated in a model of hyperlipidemia. PPP was isolated from NHPs on a standard chow diet (n = 6, lean) or NHPs on a high-fat diet (n = 8, obese). Clotting times were measured by incubating PPP with an aPTT reagent followed by CaCl₂ to initiate clot formation (A) or by stimulating PPP with Dade Innovin Reagent to measure PT. Activated coagulation protease species, FXIa–AT and T-AT, were measured using a custom ELISA (C, D). Statistical analyses were conducted using a Mann–Whitney test or an unpaired t-test. Statistical significance is indicated by an asterisk for $P \leq .05$. Data are shown as mean ± SEM. aPTT, activated partial thrombospondin time; AT, antithrombin; ELISA, enzyme-linked immunosorbent assay; F, factor; PPP, platelet-poor plasma; PT, prothrombin time; NHP, nonhuman primate.

obese primate cohort. Akin to our observations that a function-blocking anti-FXI mAb reduced C-reactive protein levels in patients with end-stage renal disease on dialysis [22], we observed a decrease in C-reactive protein levels after 3 and continuing to 4 weeks relative to baseline (day 0) of treatment with the anti-FXI mAb, h1A6 (Figure 6A). Yet, we did not observe any additional effects of FXI therapy on the elevated plasma levels of cathepsin D, myeloperoxidase, or C5b-9 soluble terminal complement complex or on the levels of platelet- or endothelial cell–derived EVs found in this model of hyperlipidemia (Figure 6B–G).

3.5 | Effects of pharmacological targeting of FXI on endothelial inflammatory markers

Endothelial cell dysfunction is one of the hallmarks of hyperlipidemia leading to atherosclerosis. This is recapitulated in the primate model of hyperlipidemia used in the current study; we have previously shown that NHPs on a high-fat diet have increased expression of endothelial VCAM-1 compared with NHPs on a standard chow diet [30]. Using a noninvasive molecular imaging technique to quantify local VCAM-1 expression at the carotid bifurcation, we confirmed that obese primates were characterized by a positive though variable increase in endothelial cell VCAM-1 expression levels at baseline. When evaluated following 4 weeks of treatment with the anti-FXI mAb, h1A6, we found an absence of VCAM-1 signal (Figure 7A). Congruent with prior studies showing that diet-induced obesity induced a reduction in

expression of P-selectin or PS as markers of platelet activation or coagulability, respectively. Statistical analyses were conducted using an unpaired t-test, Welch's t-test, or a Mann–Whitney test. Statistical significance is indicated by an asterisk for $P < .05$. Data are shown as mean ± SEM. FITC, fluorescein isothiocyanate; FSC, forward scatter; GP, glycoprotein; NHP, nonhuman primate; PS, phosphatidylserine; PT, prothrombin time; SSC, side scatter.
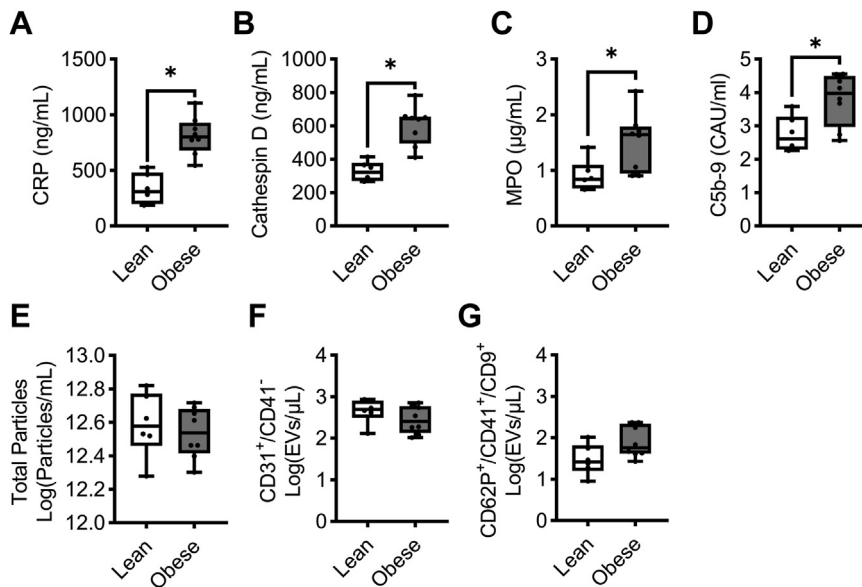
FIGURE 3 Diet-induced hyperlipidemia increased markers of systemic inflammation. PPP samples were isolated from NHPs on a standard chow diet ($n = 6$, lean) or NHPs on a high-fat diet ($n = 8$, obese). Plasma levels of C-reactive protein (A), cathepsin D (B), myeloperoxidase (C), and C5b-9 (D) in NHPs on a standard chow diet ($n = 6$, lean) or NHPs on a high-fat diet ($n = 8$, obese) were measured. For the analysis of EVs, we measured total particle concentration (E), endothelial EVs (F), or platelet EVs (G). Statistical analyses were conducted using an unpaired t-test, Welch's test, or a Mann–Whitney test. Statistical significance is indicated by an asterisk for $P < .05$. Data are shown as mean ± SEM. EV, extracellular vesicle; NHP, nonhuman primate; PPP, platelet-poor plasma.

soluble levels of VCAM-1 as compared to lean animals [30], presumably due to the fact that VCAM-1 remains endothelial cell surface associated in the setting of chronic inflammation [39], we found a decrease in circulating VCAM-1 levels in our hyperlipidemic cohort as compared to our lean cohort. Yet, the anti-FXI mAb, h1A6, was unable to reverse this trend in sVCAM-1 levels, suggesting that using sVCAM-1 as a biomarker, the ability of pharmacological targeting of FXI to acutely pacify endothelial cell VCAM-1 levels cannot be detected (Figure 7B).
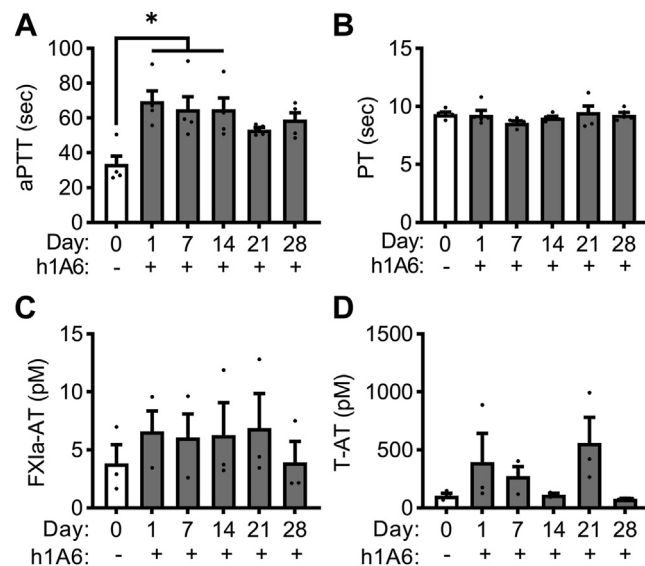
4 | DISCUSSION

This study investigated the role of FXI in sustaining thromboinflammation associated with chronic hyperlipidemia. Using a function-blocking antibody that prevented FXI activation by FXIIa as well as FIX and FV activation by FXIa, we found that pharmacological targeting of FXI reduced the levels of C-reactive protein, platelet reactivity to activation by GPVI and PAR-1 agonists, and endothelial cell activation as measured by VCAM-1 levels. These data suggest that the therapeutic effects of targeting FXI may extend beyond anti-coagulation and include antiplatelet and anti-inflammatory benefit.

Herein, we observed a selective reduction in markers of inflammation in a NHP model of diet-induced hyperlipidemia. Indeed, we found that the elevated C-reactive protein levels in an obese NHP cohort were reduced by a ~25% following 4 weeks of anti-FXI therapy. These results are consistent with the findings of Lorentz et al., which reported that administration of the anti-FXI antibody, AB023, decreased C-reactive protein levels and also attenuated T-AT levels in patients with end-stage renal disease on hemodialysis [22]. Along these lines, preliminary results from our clinical trial evaluating FXI inhibition for prevention of catheter-associated thrombosis also found that treatment with AB023 blunted the increased levels of C-reactive protein as well as T-AT levels following central line placement [40]. The efficacy of FXI inhibition observed in those studies may be in part attributed to the mechanism of action by which medical devices activate FXII to initiate thrombin generation in a FXI-dependent
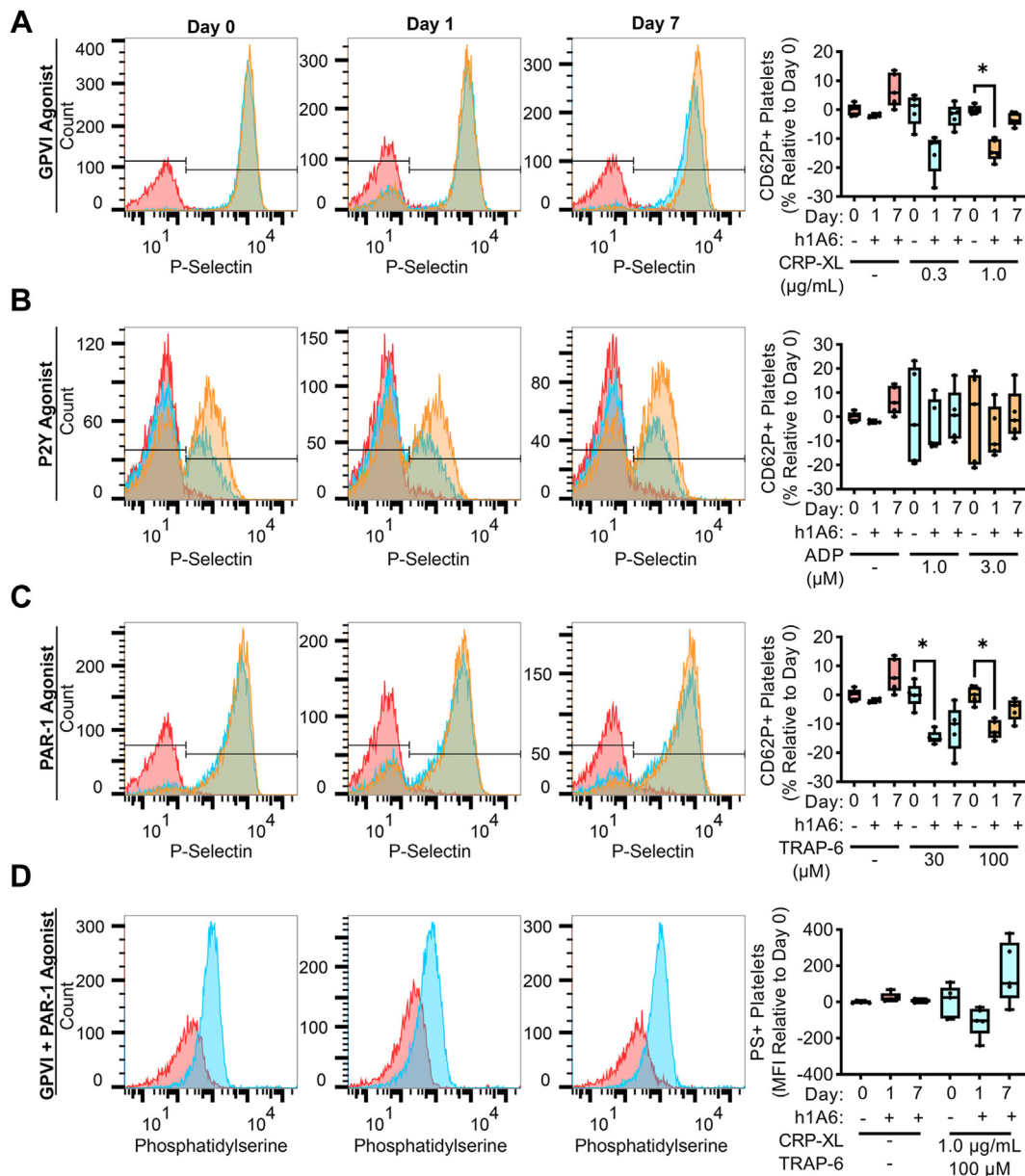

FIGURE 4 FXI inhibition prolonged aPTT clotting times in a model of hyperlipidemia. PPP was isolated from NHPs on a high-fat diet ($n = 5$) treated with a FXI function–blocking antibody. Clotting times were measured by incubating PPP with an aPTT reagent followed by $CaCl_2$ to initiate clot formation (A) or by stimulating PPP with Dade Innovin Reagent to measure PT (B). Activated coagulation protease species, FXIa–AT and T–AT, were measured using a custom ELISA (C, D). Statistical analyses were conducted using a Friedman test with a Dunn's *post-hoc* test or repeated measures one-way ANOVA with a Dunnett's *post-hoc* test. Statistical significance is indicated by an asterisk for $P < .05$. Data are shown as mean ± SEM. aPTT, activated partial thrombospondin time; AT, antithrombin; ELISA, enzyme-linked immunosorbent assay; F, factor; NHP, nonhuman primate; PPP, platelet-poor plasma; PT, prothrombin time.

FIGURE 5 The sensitization of platelets for activation by GPVI or PAR-1 agonists in the setting of hyperlipidemia was reversed following treatment with a FXI inhibitor. Whole blood samples from NHPs on a high-fat diet (*n* = 5) were stained with an anti-CD62P PE antibody (A–C) or FITC bovine lactadherin (D). Samples were then stimulated with a GPVI agonist (0.3, 1.0 μg/mL), a P2Y agonist (1.0, 3.0 μM), or a PAR-1 agonist (30, 100 μM). Flow cytometry was used to measure platelet surface expression of P-selectin and PS as markers of platelet activation or coagulability, respectively. Statistical analyses were conducted using a mixed-effects analysis with Geisser–Greenhouse correction or a Friedman test with a Dunn's *post-hoc* test. Statistical significance is indicated by an asterisk for *P* < .05. Data are shown as mean ± SEM. F, factor; FITC, fluorescein isothiocyanate; FSC, forward scatter; GP, glycoprotein; NHP, nonhuman primate; SSC, side scatter.

manner. The mechanism of action of the procoagulant and inflammatory phenotype observed in the setting of hyperlipidemia is perhaps multifaceted and includes several inciting factors, including tissue factor expressed on inflamed endothelium and circulating leukocyte or EVs. Along the lines of T-AT levels being insensitive to FXI inhibition in this model, the markers of activated leukocytes including elevated levels of cathepsin D and MPO observed in the obese NHP cohort were not affected by treatment with the anti-FXI

antibody. It appears that FXI inhibition was unable to reduce the baseline levels of procoagulant and select inflammatory activity in this model of hyperlipemia.

While C-reactive protein is a useful biomarker for inflammation, the either direct or indirect mechanisms by which C-reactive protein levels are regulated or related to FXIa activity remain to be defined. Perhaps a partial explanation lies in the crosstalk between FXI, inflammation, and the complement cascade. Indeed, we have
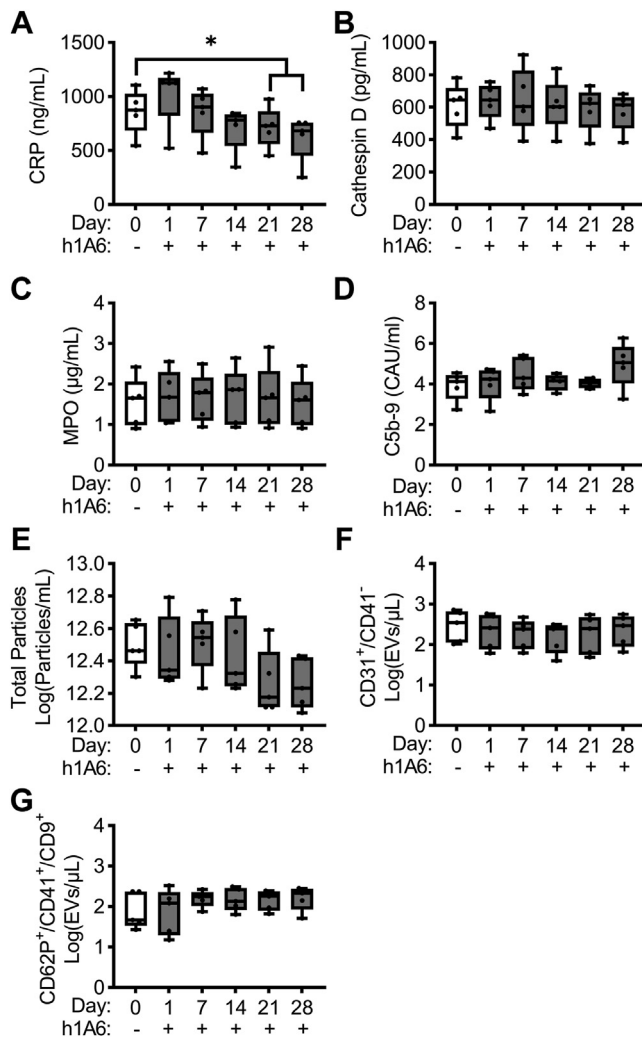
FIGURE 6 FXI inhibition prevented the increase in C-reactive protein levels in a model of hyperlipidemia. PPP was isolated from NHPs on a high-fat diet (n = 5) treated with a FXI function–blocking antibody. Plasma levels of C-reactive protein (A), cathepsin D (B), myeloperoxidase (C), and C5b-9 (D) in NHPs on a high-fat diet (n = 5) treated with a FXI function–blocking antibody were measured. For the analysis of extracellular vesicles, we measured total particle concentration (E), endothelial EVs (F), or platelet EVs (G). Data presented at day 0 served as the baseline for comparison, allowing us to establish a reference point for evaluating the effects of FXI inhibition. Statistical analyses were conducted using repeated measures one-way ANOVA with a Dunnett's *post-hoc* test or a Friedman test with a Dunn's *post-hoc* test. Statistical significance is indicated by an asterisk for $P < .05$. Data are shown as mean ± SEM. CRP, C-reactive protein; EVs, extracellular vesicles; F, factor; NHP, nonhuman primate; MPO, myeloperoxidase; PPP, platelet-poor plasma.

previously shown that FXIa neutralizes complement factor H (CFH) by specific cleavage of the R341/R342 bonds, leading to enhanced cleavage of complement components, including C3b [41]. This may in part explain why inhibiting either FXI or FXII activation in a baboon model of systemic inflammatory response syndrome prevented complement activation including C3b and C5b-9 [12,20]. As CFH is known to bind C-reactive protein to attenuate its proinflammatory

activity [42], perhaps inhibiting FXI with h1A6 disturbed the cross-talk between CFH and C-reactive protein, as well as activation of the complement cascade. Taken together, the reduction in C-reactive protein levels may represent both a biomarker and a mechanism for the anti-inflammatory effects observed following the blockade of FXI. Additionally, platelet inhibitors (eg, clopidogrel and eptifibatide) have been shown to provide an anti-inflammatory benefit in patients, including the reduction of C-reactive protein levels [43]. It may be that the antiplatelet effects of FXI inhibition likewise cause a reduction in inflammatory markers, including C-reactive protein.

By way of accelerating and propagating thrombin generation, we have shown that FXI promotes platelet activation and single platelet consumption in shear flow [44]. For instance, in a NHP model of thrombus formation on a collagen-coated vascular graft, we found that pharmacological inhibition of FXIa activation of FIX with h1A6 reduced single platelet consumption in the bloodstream distal to a site of thrombus formation [44]. This mechanism was conserved in a baboon model of systemic inflammatory response syndrome, where inhibition of FXI activation by FXIIa prevented *Staphylococcus aureus*–induced platelet and fibrinogen consumption [21]. Along these lines, the current study demonstrates that pharmacological targeting of FXI with h1A6 reduced platelet reactivity, as measured by the expression of P-selectin in response to GPVI and PAR-1 agonists, in a NHP model of hyperlipidemia. Given the variable expression of platelet P-selectin in response to a P2Y1 agonist, future studies may benefit from measuring additional markers of platelet activation (eg, GPIIb/IIIa). It is important to highlight that while the interaction of FXIa with the platelet surface may induce an allosteric modulation of FXIa, our previous experiments demonstrate that these anti-FXI monoclonal antibodies do not exhibit any observable effects on FXI–platelet binding or activation [45–47]. Moreover, since platelets provide a procoagulant surface to amplify and propagate thrombin generation, perhaps pharmacological targeting of FXI produces an antiplatelet benefit via both direct and indirect means.

By serving to facilitate adhesion and transmigration of inflammatory cells to sites of endothelial cell damage or dysfunction, VCAM-1 represents both a proinflammatory biomarker and perhaps even a therapeutic target for vascular diseases including atherosclerosis. Endothelial cell VCAM-1 expression is known to be induced by angiotensin II and thrombin [48,49]. More recently, Kossman et al. described a role for thrombin-mediated FXI activation in potentiating vascular inflammation and dysfunction in a rodent model of arterial hypertension [49]. Moreover, while FXIa can directly bind and be internalized by the vascular endothelium [50], there may be signaling mechanisms downstream that depend on FXIa beyond its role in amplifying thrombin generation. Indeed, endothelial cell inactivation of FXIa may indirectly regulate endothelial barrier function by way of activation of the membrane-bound metalloproteinase, ADAM10. This proposed mechanism may explain our prior observation that pharmacological targeting of FXI preserved endothelial barrier function in a murine model of atherogenesis [14], herein reducing endothelial cell VCAM-1 expression in nonhuman primate model of hyperlipidemia associated with early atherosclerosis.

FIGURE 7 Treatment with a FXI
inhibitor reduced VCAM-1 expression at the
inflamed vessel wall surface in the setting of
hyperlipidemia. We used a noninvasive
ultrasound-based molecular imaging
technique to measure VCAM-1 expression
at the vessel wall surface as a marker of
local activation in NHPs on a high-fat diet
(n = 5) treated with a FXI function–blocking
antibody. Data are presented as box and
whisker plots showing the background
subtracted video intensity for control and
VCAM-1-targeted microbubbles (A).
Systemic activation was determined by
measuring the circulating levels of VCAM-1
(sVCAM-1) in both NHPs on a standard
chow diet (lean) and NHPs on a high-fat diet
(obese) treated with a FXI function–blocking
antibody (B). Statistical analyses were
conducted using a Wilcoxon test, an
unpaired t-test, or a Friedman test with a
Dunn's post-hoc test. Statistical significance
is indicated by an asterisk for P < .05. Data
are shown as mean ± SEM. F, factor; NHP,
nonhuman primate; VCAM-1, vascular cell
adhesion molecule 1.
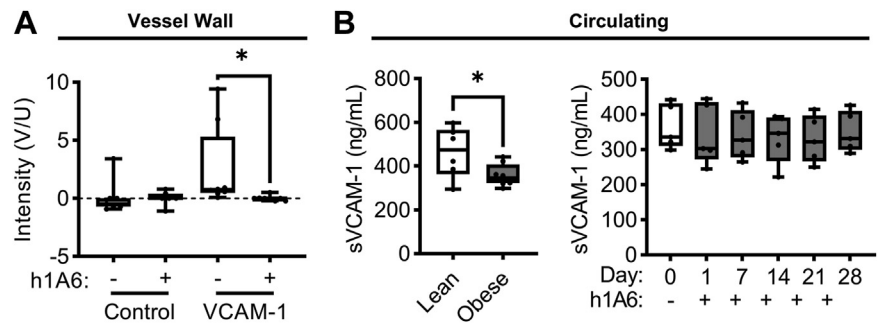
To evaluate coagulation activation, we measured aPTT, PT, FXIa–AT, and T–AT complexes. Following treatment with h1A6, we observed prolonged aPTT clotting times of up to day 14 posttreatment. Despite the maintenance dose of h1A6 following the day 14 blood draw and the unexplained elevation in T-AT levels at day 21, the aPTT prolongation did not reach statistical significance on days 21 and 28. This inconsistency may be attributed to a usually high aPTT measured for one of the animals in the day 0 group. Unfortunately, due to limited sample volume, we were not able to measure additional serine–protease complexes. Moreover, an additional limitation of our study was that we solely measured FXIa–AT complexes and did not include a broader collection of inhibitory complexes including FXIa–C1 esterase inhibitor, FXIa–alpha-1-antitrypsin, or FXIa–alpha 2-antiplasmin complexes; this decision was largely based on our prior experience of robustness and reproducibility of measuring FXIa–AT complexes in NHP plasma [12,20]. Although our findings provide insights into the role of FXIa activity in the setting of diet-induced hyperlipidemia, future work would benefit from assessing downstream effects of FXIa activity, including the activation of FIX as measured by FIX–AT levels.

Our study has several limitations. One of the limitations is that this work was designed as a composite study comprised of 2 parts: one comparing lean vs obese NHPs and the other examining the effect of inhibition of FXI. This experimental design choice was largely due to a scarcity of resources available to study NHP models of hyperlipidemia. Thus, the small sample size allowed us to neither evaluate inhibition of FXI in the lean cohort nor account for sex or age as biological variables. Indeed, only male NHPs were used in these studies, as

nonhuman primates are recognized by the National Institute of Health as an "acutely scarce resource," with females being prioritized for breeding. Additionally, NHPs in the lean cohort were significantly younger on average than NHPs in the obese cohort (8.2 vs 18.6 years, P < .0001). An additional limitation of this study is the use of a single pharmacological agent, h1A6, for these studies. As FXIa has been shown to act on substrates involved in the regulation of inflammation, platelet activation, barrier function, and the immune response, a comprehensive understanding of the role of FXI in hyperlipidemia-induced thromboinflammation will require use of additional tools including reducing FXI levels and targeting of the active site of FXIa. Even taking these limitations into account, our findings indicate that FXI may represent a safe therapeutic target to quell the thromboinflammatory mechanisms that promote atherogenesis.

AUTHOR CONTRIBUTIONS

T.C.L.K., K.R.J., M.T.H., J.J.S., C.P., and O.J.T.M. were responsible for project concept and design. M.T.H., P.K., and J.R.L. executed primate studies. T.C.L.K., I.P.-I., H.V., K.R.J., C.P., T.K.M., S.T.Y., and T.T.M.N. contributed to in vitro data acquisition and analysis. T.C.L.K. drafted the manuscript. P.K., J.E.A., M.W., C.U.L., E.I.T., D.G., and O.J.T.M. critically reviewed the manuscript.

FUNDING

TWITTER

Iván Parra-Izquierdo 🐦 @IvanParraIzq

Joseph J. Shatzel 🐦 @Clotmaster

Thuy T.M. Ngo 🐦 @ThuyMinhNgo

Joseph E. Aslan 🐦 @JoePlatelet

Erik I. Tucker 🐦 @clotguru

Jonathan R. Lindner 🐦 @JLindnerMD

REFERENCES

[1] Herrington W, Lacey B, Sherliker P, Armitage J, Lewington S. Epidemiology of atherosclerosis and the potential to reduce the global burden of atherothrombotic disease. *Circ Res.* 2016;118:535–46.

[2] Geovanini GR, Libby P. Atherosclerosis and inflammation: overview and updates. *Clin Sci (Lond).* 2018;132:1243–52.

[3] Quillard T, Franck G, Mawson T, Folco E, Libby P. Mechanisms of erosion of atherosclerotic plaques. *Curr Opin Lipidol.* 2017;28:434–41.

[4] Viola J, Soehnlein O. Atherosclerosis – a matter of unresolved inflammation. *Semin Immunol.* 2015;27:184–93.

[5] Moriya J. Critical roles of inflammation in atherosclerosis. *J Cardiol.* 2019;73:22–7.

[6] Jing L, Shu-Xu D, Yong-Xin R. A review: pathological and molecular biological study on atherosclerosis. *Clin Chim Acta.* 2022;531:217–22.

[7] Zieleniewska NA, Kazberuk M, Chlabicz M, Eljaszewicz A, Kamiński K. Trained immunity as a trigger for atherosclerotic cardiovascular disease—a literature review. *J Clin Med.* 2022;11:3369.

[8] Posma JJ, Posthuma JJ, Spronk HM. Coagulation and non-coagulation effects of thrombin. *J Thromb Haemost.* 2016;14:1908–16.

[9] d'Alessandro E, Becker C, Bergmeier W, Bode C, Bourne JH, Brown H, et al. Thrombo-inflammation in cardiovascular disease: an expert consensus document from the third Maastricht consensus conference on thrombosis. *Thromb Haemost.* 2020;120:538–64.

[10] Puy C, Tucker EI, Ivanov IS, Gailani D, Smith SA, Morrissey JH, et al. Platelet-derived short-chain polyphosphates enhance the inactivation of tissue factor pathway inhibitor by activated coagulation factor XI. *PLoS One.* 2016;11:e0165172. https://doi.org/10.1371/journal.pone.0165172

[11] Puy C, Tucker EI, Matafonov A, Cheng Q, Zientek KD, Gailani D, et al. Activated factor XI increases the procoagulant activity of the extrinsic pathway by inactivating tissue factor pathway inhibitor. *Blood.* 2015;125:1488–96.

[12] Silasi R, Keshari RS, Lupu C, Van Rensburg WJ, Chaaban H, Regmi G, et al. Inhibition of contact-mediated activation of factor XI protects baboons against S aureus-induced organ damage and death. *Blood Adv.* 2019;3:658–69.

[13] Lira AL, Kohs TCL, Moellmer SA, Shatzel JJ, Mccarty OJT, Puy C. Substrates, cofactors, and cellular targets of coagulation factor XIa. *Semin Thromb Hemost.* 2023. https://doi.org/10.1055/s-0043-1764469. in press.

[14] Ngo ATP, Jordan KR, Mueller PA, Hagen MW, Reitsma SE, Puy C, et al. Pharmacological targeting of coagulation factor XI mitigates the development of experimental atherosclerosis in low-density lipoprotein receptor-deficient mice. *J Thromb Haemost.* 2021;19:1001–17.

[15] Bane Jr CE, Ivanov I, Matafonov A, Boyd KL, Cheng Q, Sherwood ER, et al. Factor XI deficiency alters the cytokine response and activation of contact proteases during polymicrobial sepsis in mice. *PLoS One.* 2016;11:e0152968. https://doi.org/10.1371/journal.pone.0152968

[16] Luo D, Szaba FM, Kummer LW, Johnson LL, Tucker EI, Gruber A, et al. Factor XI-deficient mice display reduced inflammation, coagulopathy, and bacterial growth during listeriosis. *Infect Immun.* 2012;80:91–9.

[17] Tucker EI, Verbout NG, Leung PY, Hurst S, McCarty OJ, Gailani D, et al. Inhibition of factor XI activation attenuates inflammation and coagulopathy while improving the survival of mouse polymicrobial sepsis. *Blood.* 2012;119:4762–8.

[18] Leung PY, Hurst S, Berny-Lang MA, Verbout NG, Gailani D, Tucker EI, et al. Inhibition of factor XII-mediated activation of factor XI provides protection against experimental acute ischemic stroke in mice. *Transl Stroke Res.* 2012;3:381–9.

[19] Lorentz CU, Verbout NG, Cao Z, Liu L, Hinds MT, McCarty OJT, et al. Factor XI contributes to myocardial ischemia-reperfusion injury in mice. *Blood Adv.* 2018;2:85–8.

[20] Silasi R, Keshari RS, Regmi G, Lupu C, Georgescu C, Simmons JH, et al. Factor XII plays a pathogenic role in organ failure and death in baboons challenged with *Staphylococcus aureus*. *Blood.* 2021;138:178–89.

[21] Zilberman-Rudenko J, Reitsma SE, Puy C, Rigg RA, Smith SA, Tucker EI, et al. Factor XII activation promotes platelet consumption in the presence of bacterial-type long-chain polyphosphate in vitro and in vivo. *Arterioscler Thromb Vasc Biol.* 2018;38:1748–60.

[22] Lorentz CU, Tucker EI, Verbout NG, Shatzel JJ, Olson SR, Markway BD, et al. The contact activation inhibitor AB023 in heparin-free hemodialysis: results of a randomized phase 2 clinical trial. *Blood.* 2021;138:2173–84.

[23] Tucker EI, Marzec UM, White TC, Hurst S, Rugonyi S, McCarty OJ, et al. Prevention of vascular graft occlusion and thrombus-associated thrombin generation by inhibition of factor XI. *Blood.* 2009;113:936–44.

[24] Sanchez J, Elgue G, Riesenfeld J, Olsson P. Studies of adsorption, activation, and inhibition of factor XII on immobilized heparin. *Thromb Res.* 1998;89:41–50.

[25] Keshari RS, Silasi R, Popescu NI, Patel MM, Chaaban H, Lupu C, et al. Inhibition of complement C5 protects against organ failure and reduces mortality in a baboon model of *Escherichia coli* sepsis. *Proc Natl Acad Sci U S A.* 2017;114:e6390–9. https://doi.org/10.1073/pnas.1706818114

[26] Clemente L, Boeldt DS, Grummer MA, Morita M, Morgan TK, Wiepz GJ, et al. Adenoviral transduction of EGFR into pregnancy-adapted uterine artery endothelial cells remaps growth factor induction of endothelial dysfunction. *Mol Cell Endocrinol.* 2020;499:110590.

[27] Kuhn M, Zhang Y, Favate J, Morita M, Blucher A, Das S, et al. IMP1/IGF2BP1 in human colorectal cancer extracellular vesicles. *Am J Physiol Gastrointest Liver Physiol.* 2022;323:G571–85. https://doi.org/10.1152/ajpgi.00121.2022

[28] Mitrugno A, Tassi Yunga S, Sylman JL, Zilberman-Rudenko J, Shirai T, Hebert JF, et al. The role of coagulation and platelets in colon cancer-associated thrombosis. *Am J Physiol Cell Physiol.* 2019;316:C264–73. https://doi.org/10.1152/ajpcell.00367.2018

[29] Brown E, Ozawa K, Moccetti F, Vinson A, Hodovan J, Nguyen TA, et al. Arterial platelet adhesion in atherosclerosis-prone arteries of obese, insulin-resistant nonhuman primates. *J Am Heart Assoc.* 2021;10:e019413. https://doi.org/10.1161/JAHA.120.019413

[30] Chadderdon SM, Belcik JT, Bader L, Kirigiti MA, Peters DM, Kievit P, et al. Proinflammatory endothelial activation detected by molecular imaging in obese nonhuman primates coincides with onset of insulin resistance and progressively increases with duration of insulin resistance. *Circulation.* 2014;129:471–8.

[31] Kohs TCL, Olson SR, Pang J, Jordan KR, Zheng TJ, Xie A, et al. Ibrutinib inhibits BMX-dependent endothelial VCAM-1 expression in vitro and pro-atherosclerotic endothelial activation and platelet adhesion in vivo. *Cell Mol Bioeng.* 2022;15:231–43.

[32] Rigg RA, Aslan JE, Healy LD, Wallisch M, Thierheimer ML, Loren CP, et al. Oral administration of Bruton's tyrosine kinase inhibitors impairs GPVI-mediated platelet function. *Am J Physiol Cell Physiol.* 2016;310:C373–80. https://doi.org/10.1152/ajpcell.00325.2015

[33] Zheng TJ, Lofurno ER, Melrose AR, Lakshmanan HHS, Pang J, Phillips KG, et al. Assessment of the effects of Syk and BTK inhibitors on GPVI-mediated platelet signaling and function. *Am J Physiol Cell Physiol.* 2021;320:C902–15. https://doi.org/10.1152/ajpcell.00296.2020

[34] Kay JG, Grinstein S. Phosphatidylserine-mediated cellular signaling. *Adv Exp Med Biol.* 2013;991:177–93.

[35] Vance JE, Steenbergen R. Metabolism and functions of phosphatidylserine. *Prog Lipid Res.* 2005;44:207–34.

[36] Zheng TJ, Kohs TCL, Mueller PA, Pang J, Reitsma SE, Parra-Izquierdo I, et al. Effect of antiplatelet agents and tyrosine kinase inhibitors on oxLDL-mediated procoagulant platelet activity. *Blood Adv.* 2023;7:1366–78.

[37] Ellulu MS, Patimah I, Khaza'ai H, Rahmat A, Abed Y. Obesity and inflammation: the linking mechanism and the complications. *Arch Med Sci.* 2017;13:851–63.

[38] Hotamisligil GS. Inflammation and metabolic disorders. *Nature.* 2006;444:860–7.

[39] Videm V, Albrigtsen M. Soluble ICAM-1 and VCAM-1 as markers of endothelial activation. *Scand J Immunol.* 2008;67:523–31.

[40] Pfeffer MA, Vu H, Kohs TC, Wang J, Lorentz CU, Tucker EI, et al. Factor XI inhibition for the prevention of catheter-associated thrombosis in cancer patients undergoing central line placement: a phase 2 clinical trial. *Blood.* 2022;140:1247–9.

[41] Puy C, Pang J, Reitsma SE, Lorentz CU, Tucker EI, Gailani D, et al. Cross-talk between the complement pathway and the contact activation system of coagulation: activated factor XI neutralizes complement factor H. *J Immunol.* 2021;206:1784–92.

[42] Molins B, Fuentes-Prior P, Adán A, Antón R, Arostegui JI, Yagüe J, et al. Complement factor H binding of monomeric C-reactive protein downregulates proinflammatory activity and is impaired with at risk polymorphic CFH variants. *Sci Rep.* 2016;6:22889.

[43] Prasad K. C-reactive protein (CRP)-lowering agents. *Cardiovasc Drug Rev.* 2006;24:33–50.

[44] Zilberman-Rudenko J, Itakura A, Wiesenekker CP, Vetter R, Maas C, Gailani D, et al. Coagulation factor XI promotes distal platelet activation and single platelet consumption in the bloodstream under shear flow. *Arterioscler Thromb Vasc Biol.* 2016;36:510–7.

[45] Cheng Q, Tucker EI, Pine MS, Sisler I, Matafonov A, Sun MF, et al. A role for factor XIIa-mediated factor XI activation in thrombus formation in vivo. *Blood.* 2010;116:3981–9.

[46] Reitsma SE, Pang J, Raghunathan V, Shatzel JJ, Lorentz CU, Tucker EI, et al. Role of platelets in regulating activated coagulation factor XI activity. *Am J Physiol Cell Physiol.* 2021;320:C365–74. https://doi.org/10.1152/ajpcell.00056.2020

[47] White-Adams TC, Berny MA, Tucker EI, Gertz JM, Gailani D, Urbanus RT, et al. Identification of coagulation factor XI as a ligand for platelet apolipoprotein E receptor 2 (ApoER2). *Arterioscler Thromb Vasc Biol.* 2009;29:1602–7.

[48] Kaplanski G, Marin V, Fabrigoule M, Boulay V, Benoliel AM, Bongrand P, et al. Thrombin-activated human endothelial cells support monocyte adhesion in vitro following expression of intercellular adhesion molecule-1 (ICAM-1; CD54) and vascular cell adhesion molecule-1 (VCAM-1; CD106). *Blood.* 1998;92:1259–67.

[49] Kossmann S, Lagrange J, Jäckel S, Jurk K, Ehlken M, Schönfelder T, et al. Platelet-localized FXI promotes a vascular coagulation-inflammatory circuit in arterial hypertension. *Sci Transl Med.* 2017;9:eaah4923. https://doi.org/10.1126/scitranslmed.aah4923

[50] Puy C, Ngo ATP, Pang J, Keshari RS, Hagen MW, Hinds MT, et al. Endothelial PAI-1 (plasminogen activator inhibitor-1) blocks the intrinsic pathway of coagulation, inducing the clearance and degradation of FXIa (activated factor XI). *Arterioscler Thromb Vasc Biol.* 2019;39:1390–401.

SUPPLEMENTARY MATERIAL

The online version contains supplementary material available at https://doi.org/10.1016/j.rpth.2023.102276